Organic Geochemistry 159 (2021) 104275

Contents lists available at ScienceDirect

Organic Geochemistry

journal homepage: www.elsevier.com/locate/orggeochem

Organic compounds in vent fluids from Yellowstone Lake, Wyoming

Claire Ong [a], Andrew P.G. Fowler [b], William E. Seyfried Jr. [b], Tao Sun [c], Qi Fu [a,*]

[a] Department of Earth and Atmospheric Sciences, University of Houston, Houston, TX 77204, USA
[b] Department of Earth and Environmental Sciences, University of Minnesota, Minneapolis, MN 55455, USA
[c] Department of Earth, Environmental and Planetary Sciences, Rice University, Houston, TX 77005, USA

ARTICLE INFO

Associate Editor–**Kliti Grice**

Keywords:
Yellowstone Lake
Organic compounds
Hydrothermal fluids
Fluid-rock interaction
Carbon isotopes

ABSTRACT

Hydrothermal fluids were collected over a three-year interval (2016–2018) from two sublacustrine vent fields in Yellowstone Lake, Wyoming: Stevenson Island Deep Hole (YL16 and YL17 series in 2016 and 2017, respectively) and West Thumb (YL18 series in 2018). The TOC content in SI Deep Hole vent fluids varies from 2.7 mg/L to 6.3 mg/L in YL16 and 5.0 mg/L to 16.2 mg/L in YL17. Compared to YL16, the average TOC value of YL17 has more than doubled. The range of TOC is from 7.3 mg/L to 13.7 mg/L in the West Thumb samples. A positive correlation between TOC and dissolved CO_2 concentration is observed in most samples, suggesting their close relationship with sublacustrine heat and mass transfer processes. The organic compounds detected at both vent fields are diverse in molecular structure. In the SI Deep Hole, complex cyclic and unsaturated organic compounds are dominant, with cyclic hydrocarbons having the highest abundance, followed by carboxylic acids, PAHs, and alcohols. At West Thumb vents, propanol is most abundant, followed by alcohols, PAHs, alkanes, and carboxylic acids. This difference in structural complexity and relative quantity of organic compounds may be attributed to the involvement of hydrothermal processes. The vapor-dominated hydrothermal system and extensive fluid-rock interactions in SI Deep Hole facilitate alteration/decomposition of organic precursors. While $CO_{2(aq)}$ is predominant in vent fluids, dissolved CH_4 is much less abundant. In SI Deep Hole, the carbon isotopic composition of CH_4 in most samples ranges from −20.4‰ to −38.0‰, with values of less than −60‰ in three samples, while CO_2 ranges from −4.4‰ to −10.5‰. A temporal variation of $\delta^{13}C$ values was obtained for CO_2, with the average increasing from −9.2‰ (YL16) to −5.2‰ (YL17). In West Thumb, the $\delta^{13}C$ value of CO_2 and CH_4 fall in a similar range, with an average of −10.5‰ and −19.0‰, respectively. There are multiple sources for observed carbon species: the interaction of vent fluids with subsurface rocks and lake sediments is the predominant process, followed by thermal decomposition of organic matter. Microbial activity on the lake floor may contribute to methane formation, while magmatic degassing is the major process that produces CO_2. The connection between vapor-dominated hydrothermal alteration, elevated TOC contents and dissolved CO_2 in vent fluids, and enrichment of ^{13}C in CO_2 in YL17 in SI Deep Hole suggests an interplay of geological, chemical, and biological processes and their imprints on vent fluids, all of which make significant contribution to the carbon cycle in the Yellowstone Lake ecosystem.

1. Introduction

Yellowstone Lake in Wyoming, USA is the largest high altitude lake in North America, located in the southeast region of the Yellowstone caldera. Within the Yellowstone Plateau Volcanic Field (YPVF), three major volcanic episodes contributed to the development of the Yellowstone caldera, which are recorded by deposits of the Huckleberry Ridge Tuff (2.06 Ma), Mesa Falls Tuff (1.29 Ma), and Lava Creek Tuff (0.64 Ma) (Christiansen and Blank, 1972; Christiansen, 1984, 2001; Lanphere et al., 2002). A minor eruption, at about 147 ka, created the West Thumb caldera, on the southwest margin of Yellowstone Lake (Fritz, 1985; Christiansen, 2001).

More than 250 hydrothermal vents have been identified on the floor of Yellowstone Lake (Morgan et al., 2003). The vent fluids contain alkali metals, alkaline earth metals, and other trace elements (As, B, Cu, Ge, Hg, Mo, Sb, W), in addition to major anions (Cl^-, HCO_3^-, and SO_4^{2-}) (Shanks et al., 2005, 2007; Balistrieri et al., 2007; Gemery-Hill et al., 2007; Fowler et al., 2019a,b). The formation of vent fluids is attributed

* Corresponding author.
E-mail address: qfu5@central.uh.edu (Q. Fu).

https://doi.org/10.1016/j.orggeochem.2021.104275
Received 13 February 2021; Received in revised form 29 June 2021; Accepted 6 July 2021
Available online 12 July 2021

to the interaction between meteoric water, igneous and sedimentary rock formations, and volcanic gases, that is enhanced by high heat flow (White et al., 1988; Fournier, 1989; Sohn et al., 2019). Owing to the variability of sublacustrine hydrothermal venting, different regions of the lake often express subtle, but still significant differences in lake water chemistry. For example, the vents at West Thumb contain relatively elevated concentrations of Cl^- (50–1150 μM) and HCO_3^- (510–3040 μM), whereas the vents near Stevenson Island yield higher proportions of H_2S, which accounts for the noteworthy dissolved SO_4^{2-} in the near vent lake water (Balistrieri et al., 2007). Recent high-resolution sampling has further revealed that the chemical diversity and governing processes rival those of their subaerial counterparts (Fowler et al., 2019a).

The spatial variation of vent fluid chemistry is a manifestation of the linkage between diverse physicochemical conditions (temperature, pH, and redox) of hydrothermal vents and a suite of sublacustrine processes involving vent fluids. Those processes may include reacting with rhyolitic rocks, limestones, and sediments buried in the caldera; boiling; and steam mixing with lake water prior to venting (Klump et al., 1988; Sheppard et al., 1992; Werner and Brantley, 2003; Tan et al., 2017; Fowler et al., 2019a,b). In particular, recent studies have shown distinct hydrothermal processes with prominent chemical and mineralogical heterogeneity in vent fluids and deposits between two sublacustrine hydrothermal fields: Stevenson Island Deep Hole (SI Deep Hole) and West Thumb (Fowler et al., 2019a,b).

Vent fluids issuing from SI Deep Hole have chemical compositions similar to Yellowstone lake water, since vapor addition dominates heat and mass transport processes. Accordingly, these vent fluids can be classified as the "carbonic-acid-sulfide" type with elevated CO_2 and H_2S inherited from the steam source (Fowler et al., 2019a,b). They are formed from condensation of steam on contact with cold lake water at temperatures in excess of 175 °C at the lake bottom pressure. The low silica content derived from acidic conversion of kaolinite to boehmite precludes the formation of constructional deposits. In contrast, West Thumb vent fluids are moderately rich in chloride, and formed from the binary mixing of Cl-poor meteoric water with high temperature (345–364 °C) Cl-bearing thermal fluids at depth beneath the lake floor (Fowler et al., 2019a; Tudor et al., 2021). The fluids are neutral in pH and often associated with siliceous deposits. They are similar to alkaline-chloride fluids that are abundant in subaerial geyser basins of Yellowstone, but with lower pH values due to high hydrostatic pressure at the lake bottom, which enhances CO_2 solubility.

The immediate coupling of physical, chemical, and biological processes in YPVF fosters the development of the Yellowstone ecosystem. Biodiversity and organic composition have been extensively evaluated in geysers, fumaroles, and subaerial thermal springs in this area (Des Marais et al., 1981; Clifton et al., 1990; Barns et al., 1994; Reysenbach et al., 2000; Inskeep et al., 2005; Meyer-Dombard et al., 2005; Walker et al., 2005; Moran et al., 2017; Gonsior et al., 2018). Prior studies have also shown the abundance of microbial and biological communities in sublacustrine vents in Yellowstone Lake, a spatially distinct hydrothermal environment (Klump et al., 1988; Lovalvo et al., 2010; Clingenpeel et al., 2011; Kan et al., 2011; Yang et al., 2011; Inskeep et al., 2015). With remotely operated underwater vehicles (ROVs), observations of the floor of Yellowstone Lake at West Thumb and the deeper regions of the lake near Stevenson Island have often revealed white-colored mats/precipitates surrounding venting fissures and fumaroles that result from growth of microorganisms (Klump et al., 1988). The warm sediments on the lake floor are ideal habitats for prolific groups of autotrophic and heterotrophic microorganisms, algae, and benthic worms. The lake sediments are diatomaceous ooze consisting of up to 60% biogenic silica, with an organic carbon content of 3% (Klump et al., 1988; Shanks et al., 2007). Metagenome sequencing of vent fluids has revealed diverse microorganism communities with different populations, some of which are unique in sublacustrine areas (Inskeep et al., 2015). This diversity is directly linked to vent fluid chemistry that ultimately is attributed to associated hydrothermal processes. For example, the presence of framboidal pyrite in SI Deep Hole vents varies spatially and temporally, suggesting fluctuation of microbial sulfate reduction in the dynamic vent environment over space and time (Fowler et al., 2019c).

However, little information exists on organic components and their potential source(s) in sublacustrine vent fluids in Yellowstone Lake, which is an integral part of the hydrothermal system in YPVF. Such data are essential if a better understanding of the stability of dissolved organic compounds in hydrothermal fluids at temperature and pressure extrema is to be realized. The high hydrostatic pressure of the SI Lake floor vents in particular, effectively accounts for the high temperatures, while underscoring the importance of the samples as "windows" into processes in the root zones of more deeply seated, yet nearby, subaerial systems in Yellowstone National Park (Fowler et al., 2019a; Tan et al., 2020; Tudor et al., 2021). How these elevated temperatures and pressures impact the organic-rich substrate through which the hot, pressurized fluids pass, represents a fundamental objective of the present study.

2. Materials and methods

Fluid samples were collected from two distinct sites of hydrothermal activity on the floor of Yellowstone Lake (Fig. 1; Table 1) (Tan et al., 2017; Fowler et al., 2019a,b). The so-called Deep Hole area is located 2 km east of Stevenson Island (SI), and is the deepest region of the lake at 100–125 m depth owing to the existence of conical depressions, linearly associated with a series of NW trending fracture zones (Morgan et al., 2003, 2007, 2009; Shanks et al., 2005, 2007; Fowler et al., 2019a,b). The vents in West Thumb, the western part of Yellowstone Lake, are shallower at depths of about 50 m. In contrast to the Stevenson Island vents, the West Thumb field is aligned with siliceous ridges and mounds from which the hot fluids vent. There are two sets of samples from SI Deep Hole (YL16 and YL17), with a temporal gap of one year (2016 and 2017, respectively), whereas the West Thumb samples (YL18) were collected in 2018. Water samples collected distal to the vents from ambient lake water are named the Bottom Lake Water (BLW) series, and were used for comparison of the organic composition with vent fluid samples. The details of sample collection and storage methods are described in Fowler et al. (2019a,b).

Fine sediment particles in each sample were removed with a syringe filter containing polyethersulfone membrane in 0.2 μm pore size prior to analysis. The total amount of organic carbon in vent samples was measured using a Fusion Total Organic Carbon (TOC) Analyzer (Teledyne Tekmar). The method of ultraviolet persulfate oxidation was used with the detection limit of 0.2 ppb. Each result was the mean value of duplicate or triplicate analyses. The concentration of dissolved gases (CH_4 and CO_2 in particular), that were present in a separated gas phase from vent fluids following collection, was measured by gas chromatography (Agilent 6890A) with a thermal conductivity detector (TCD) and a flame ionization detector (FID) (Fowler et al., 2019a). The instrument also contained a methanizer, where CO_2 was converted to CH_4 that can be detected subsequently by FID (Porter and Volman, 1962). The temperature program for step-heating was performed as follows: 40 °C for 1.7 min, 40 °C/min to 220 °C, and 220 °C for 20 min. Head space gases (measured) were combined with Henry's Law calculations to obtain gas for the liquid fraction. The concentrations reported represent values for the combined fractions (Fowler et al., 2019a).

The identification of aqueous organic compounds was performed with a triple quadrupole high-performance liquid chromatography–mass spectrometry (HPLC–MS-MS) system (Agilent 6460), utilizing a Jet Stream ion source operated in positive mode. The mass spectrometer was connected to an Agilent 1260 Infinity quaternary LC system, which has an Agilent Hi-Plex H column (300 mm long × 7.7 mm ID, 8 μm particle size) heated at 30 °C. The analytical method, controlled by the Agilent MassHunter program, included an injection volume of 2.0 μl and a flow rate of 0.6 mL/min for the mobile phase. Solution A of the

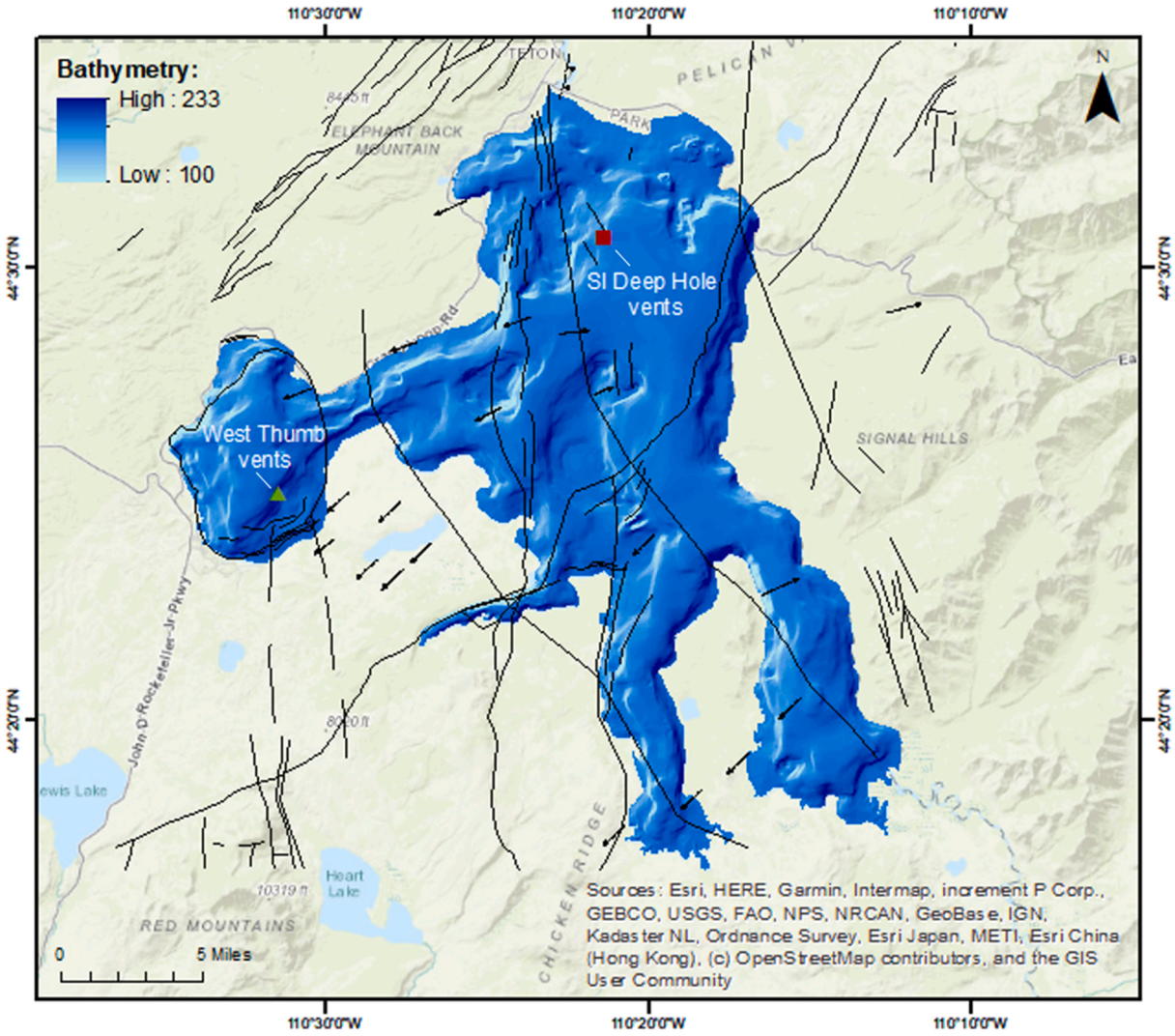

Fig. 1. Bathymetry and location of the SI Deep Hole and West Thumb hydrothermal vents in Yellowstone Lake. The latitude and longitude coordinates for each sample are listed in Table 1. The black lines and arrows show faults and flow direction of lake water, respectively.

mobile phase mixture was acetonitrile, and solution B was 0.1% formic acid. Analysis was carried out with a linear gradient from 5% A and 95% B to 95% A and 5% B in 20 min and then held for 5 min. A full scan mode over a range of m/z 50 to 1000 was selected for the second mass spectrometer to identify organic compounds. For each location (SI Deep Hole or West Thumb), the relative abundance of each organic compound was obtained by calculating the proportion of each compound's average count in mass spectra. The average count for each compound can be acquired through the summation of counts for all the samples and followed by division of that total value over the number of samples. The concentration of each organic group then can be estimated by multiplying its relative abundance by the average TOC value in each location.

The compound-specific carbon isotope analysis of gases (CO_2 and CH_4) was conducted by a gas chromatography–combustion-isotope ratio mass spectrometer (GC–C-IRMS) system. The GC (Trace GC Ultra, Thermo Scientific) was configured with a 30 m capillary PoraPLOT Q column (Agilent). It was connected to a Delta V IRMS (Thermo Scientific) through a combustion furnace running at 940 °C. The temperature step-heating program for GC started at 45 °C (held for 2 min), and ramped to 210 °C with a rate of 50 °C/min (held for 12 min). The carrier gas was UHP helium (99.999%) with flow rate of 12 mL/min. Due to the low abundance of CH_4 and use of N_2 gas in sample collection and storage, overlapping peaks of CO_2 (oxidation of CH_4) and N_2O (oxidation of N_2) were present in the chromatograms. The reference material 8560 (from National Institute of Standards and Technology) with known isotopic composition for CH_4 (−44.8‰) and CO_2 (−8.5‰), was mixed with N_2 gas in different volumes (20–80%) for calibration of carbon isotope values. The analytical error (1σ) for CH_4 varied from $\pm <$ 2‰ to 5‰, whereas it was ± 0.5‰ for CO_2. Each isotope result is the mean value of triplicate analyses.

Table 1
Fluid samples collected from SI Deep Hole and West Thumb hydrothermal vents, their location and measured temperature while sampling.

Samples	Location (Latitude, Longitude)	Sample Temperature (°C)
	SI Deep Hole	
YL16F01	44.51093, –110.35662	63
YL16F03	44.51093, –110.35662	103–120
YL16F05	44.51080, –110.35660	14–94
YL16F06	44.51090, –110.35660	96–105
YL16F07	44.51075, –110.35654	140
YL16F08	44.51075, –110.35653	110–142
YL16F10	44.51084, –110.35659	94–100
YL16F12	44.51067, –110.35660	110–114
YL16F13	44.51069, –110.35662	80–86
YL16F14	44.51069, –110.35662	137–160
YL17F01	44.51069, –110.35662	150
YL17F02	44.51069, –110.35662	141–150
YL17F03	44.51068, –110.35661	142
YL17F08	44.51069, –110.35662	115–140
YL17F10	44.51069, –110.35662	143
	West Thumb	
YL18F11	44.41639, –110.52495	141
YL18F14	44.41637, –110.52497	65–80
YL18F15	44.41638, –110.52488	36–45
YL18F17	44.41621, –110.52532	60
YL18F19	44.41637, –110.52522	65–71
	Bottom Lake Water*	
BLW 2	44.51111, –110.35659	4
BLW 3	44.51111, –110.35659	4

*lake water collected on the lake floor distal to hydrothermal vents for comparison of chemical components (see Section 2).

Table 2
The amount of total organic carbon (TOC) and dissolved CO_2* in vent fluid samples and bottom lake waters.

Samples	TOC (mg/L)	Dissolved CO_2 (mg/L)
	SI Deep Hole	
YL16F01	2.9	36
YL16F03	2.7	122
YL16F05	6.3	93
YL16F06	3.6	233
YL16F07	5.6	620
YL16F08	n.a.	331
YL16F10	n.a.	296
YL16F12	4.8	278
YL16F13	2.8	127
YL16F14	3.6	263
YL17F01	5.0	759
YL17F02	5.0	538
YL17F03	10.7	473
YL17F08	n.a.	572
YL17F10	16.2	535
	West Thumb	
YL18F11	13.7	451
YL18F14	10.2	301
YL18F15	13.4	46
YL18F17	9.0	106
YL18F19	7.3	19
	Bottom Lake Water	
BLW 2	2.7	b.d.
BLW 3	4.0	b.d.

*Data of dissolved CO_2 are from Fowler et al. (2019a).
n.a.: not available, due to limited volume for analysis.
b.d.: below detection limit.

3. Results

3.1. Total organic carbon (TOC) and dissolved CO_2

The total amount of organic carbon in vent fluids varies from 2.7 mg/L to 16.2 mg/L in the SI Deep Hole (Table 2). For the YL16 samples, the value is between 2.7 mg/L and 6.3 mg/L, with an average of 4.0 mg/L. The abundance of TOC is higher in the YL17 samples, ranging from 5.0 mg/L to 16.2 mg/L. The average TOC concentration is 9.2 mg/L, more than double the value of YL16 samples. In West Thumb, the fluids have elevated organic contents. The range of TOC concentrations is 7.3 mg/L to 13.7 mg/L, with an average of 10.7 mg/L. The bottom lake water has less organic carbon than most vent fluids, with concentrations of 2.7 mg/L and 4.0 mg/L (Table 2), confirming a hydrothermal source for organic compounds in vent fluids.

The concentration of dissolved CO_2 in vent fluids, listed in Table 2, varies significantly, while the concentration of dissolved CH_4 is notably lower (Fowler et al., 2019a). In the SI Deep Hole, the concentration ranges from 36 mg/L to 620 mg/L for the YL16 samples, and 473 mg/L to 759 mg/L for the YL17 samples which have higher $CO_{2(aq)}$ concentrations than all but one YL16 sample. The average $CO_{2(aq)}$ concentrations are 240 mg/L and 575 mg/L, respectively, for YL16 and YL17. The variation in dissolved CO_2 concentrations is notable for samples from West Thumb, ranging from 19 mg/L to 451 mg/L, with an average of 185 mg/L. The concentration of dissolved CO_2 was too low to be detected in the two bottom lake water samples, most likely due to the pH level (5.5–5.8) of lake water (Fowler et al., 2019a).

Table 3
Organic compounds identified in bottom lake water (BLW) samples collected distal to hydrothermal vents on the lake floor.

Compounds	Formula	BLW2	BLW3
Alcohols			
Propanol	C_3H_8O	×	×
Carboxylic acids			
Pyruvic acid	$C_3H_4O_3$	×	
Acetoacetic acid	$C_4H_6O_3$		×
PAHs			
Methyl naphthalene	$C_{11}H_{10}$		×

3.2. Organic compounds

3.2.1. Bottom lake water (BLW)

Only a limited number of organic groups are present in BLW samples, which include alcohols, carboxylic acids, and polycyclic aromatic hydrocarbons (PAHs) (Table 3). Those organic compounds have short straight 3- or 4-carbon chains, or simple aromatic structures. Propanol is identified in both BLW samples. Pyruvic acid exists only in BLW2, while acetoacetic acid was observed in BLW3. Methyl naphthalene is the single PAH compound in BLW3. No PAHs were identified in BLW2 (Table 3).

3.2.2. SI Deep Hole

There are more groups of organic compounds in vent fluids from SI Deep Hole than BLW (Tables 4a and 4b). Besides alcohols, carboxylic acids, and PAHs that are present in BLW, unsaturated cyclic hydrocarbons, saturated alkanes, and derivatives of benzene were also identified. For all the compounds, the number of carbon atoms are higher in SI Deep Hole, showing long chains (with branches), cyclic structures, and

Table 4a
Groups of organic compounds identified in fluids (YL16 series) from SI Deep Hole hydrothermal vents.

Compounds	Formula	YL16F01	YL16F03	YL16F05	YL16F06	YL16F07	YL16F08	YL16F10	YL16F12	YL16F13	YL16F14
Alcohols											
Propanol	C_3H_8O		×		×				×	×	
Alkanes											
Nonane	C_9H_{20}						×				
Cyclics											
Cycloheptene	C_7H_{12}					×	×	×	×	×	
Cyclooctadiene	C_8H_{12}							×		×	
Carboxylic acids											
Pyruvic acid	$C_3H_4O_3$			×		×	×		×		
Isobutyric acid	$C_4H_8O_2$	×				×					
Acetoacetic acid	$C_4H_6O_3$					×					
Malic acid	$C_4H_6O_5$							×			
Decanoic acid	$C_{10}H_{20}O_2$		×	×	×	×				×	×
PAHs											
Naphthalene	$C_{10}H_8$	×	×	×			×		×		×
Methyl naphthalene	$C_{11}H_{10}$	×									
Acenaphthene	$C_{12}H_{10}$	×	×				×			×	
Pyrene	$C_{16}H_{10}$							×			
Benzenes											
Styrene	C_8H_8					×					

Table 4b
Groups of organic compounds identified in fluids (YL17 series) from SI Deep Hole hydrothermal vents.

Compounds	Formula	YL17F01	YL17F02	YL17F03	YL17F08	YL17F10
Alcohols						
Propanol	C_3H_8O	×	×			
Alkanes						
Nonane	C_9H_{20}					
Cyclics						
Cycloheptene	C_7H_{12}					
Cyclooctadiene	C_8H_{12}					
Carboxylic acids						
Pyruvic acid	$C_3H_4O_3$	×		×	×	
Isobutyric acid	$C_4H_8O_2$			×		
Acetoacetic acid	$C_4H_6O_3$					
Malic acid	$C_4H_6O_5$					
Decanoic acid	$C_{10}H_{20}O_2$				×	
PAHs						
Naphthalene	$C_{10}H_8$	×	×	×	×	×
Methyl naphthalene	$C_{11}H_{10}$				×	
Acenaphthene	$C_{12}H_{10}$	×		×	×	
Pyrene	$C_{16}H_{10}$					
Benzenes						
Styrene	C_8H_8					

Table 5
Groups of organic compounds identified in fluids from West Thumb hydrothermal vents.

Compounds	Formula	YL18F11	YL18F14	YL18F15	YL18F17	YL18F19
Alcohols						
Propanol	C_3H_8O		×			
Alkanes						
Dodecane	$C_{12}H_{26}$		×			
Carboxylic acids						
Pyruvic acid	$C_3H_4O_3$		×		×	×
Isobutyric acid	$C_4H_8O_2$		×		×	×
PAHs						
Naphthalene	$C_{10}H_8$					×
Methyl naphthalene	$C_{11}H_{10}$	×	×	×		
Acenaphthene	$C_{12}H_{10}$	×	×		×	×
Pyrene	$C_{16}H_{10}$			×		

complex aromatic rings.

In addition to propanol, cyclic hydrocarbons were observed, including cycloheptene and cyclooctadiene. Nonane is also present in one sample.

Other than pyruvic and acetoacetic acids, the carboxylic acids identified in SI Deep Hole include isobutyric acid, malic acid, and decanoic acid, showing branched, longer, and complex structures with addition of other functional groups.

The aromatic organic compounds consist of PAHs and derivatives of benzene, which contain diverse molecular structures in addition to benzene rings. For example, acenaphthene, pyrene, and styrene have multiple benzene rings or additional functional groups.

Out of the total number of 15 samples (10 in YL16 and 5 in YL17 series) analyzed from SI Deep Hole, carboxylic acids and PAHs are the most common molecules among those organic compounds (Tables 4a and 4b). In particular, pyruvic acid, decanoic acid, naphthalene, and acenaphthene are present in half or more than half of the samples. Naphthalene was the most frequently observed compound in both the YL16 and YL17 series. The lack of alkanes, cyclic alkenes, and derivatives of benzene is noticeable in YL17 samples.

3.2.3. West Thumb

The major organic compounds present in the West Thumb vent fluid samples include carboxylic acids and PAHs (Table 5). Pyruvic and isobutyric acids are the only carboxylic acids that were observed, and they exist in more than half of the samples. For PAHs, methyl naphthalene and acenaphthene are abundant in most samples, while naphthalene and pyrene are present in only one sample. Similarly, propanol and dodecane were also identified in only one sample. Cyclic hydrocarbons were not detected in the West Thumb samples (Table 5).

No organic compounds containing heteroatoms (S, N, etc.) were identified. This is most likely attributed to the overall low abundance of TOC in these fluids. Concentrating dissolved organics with solid phase extraction (SPE) would allow for identification of more organic compounds (Hawkes et al., 2015; Gonsior et al., 2018). However, several functional groups cannot be extracted by SPE from fluids, including carboxylic acids and alcohols (Hawkes et al., 2015). The analytical approach applied and observations made in this study are intended to complement prior investigations of dissolved organic compounds in vent fluids, most of which were conducted in subaerial hydrothermal systems

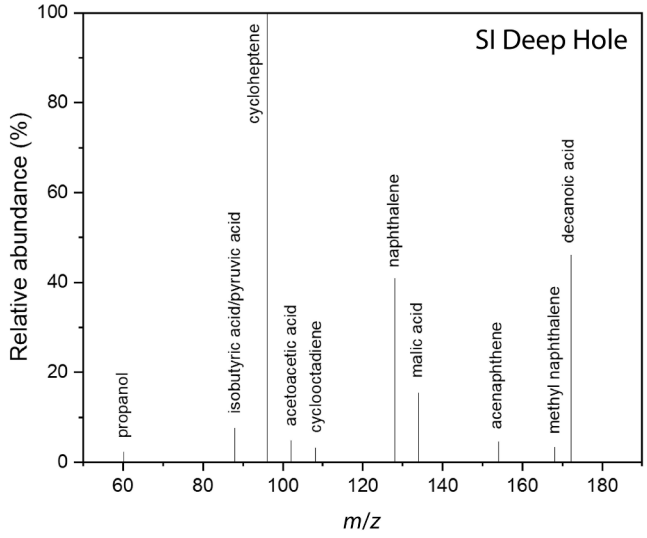

Fig. 2. Mass spectra with overlain peaks obtained by full scan mode showing major organic compounds identified in SI Deep Hole vent fluids. Combined together, cyclic hydrocarbons (43.3%) have the highest abundance, followed by carboxylic acids (36.6%), PAHs (19.3%), and alcohols (0.8%). The lack of reported nonane, pyrene, and styrene is due to extremely low abundances.

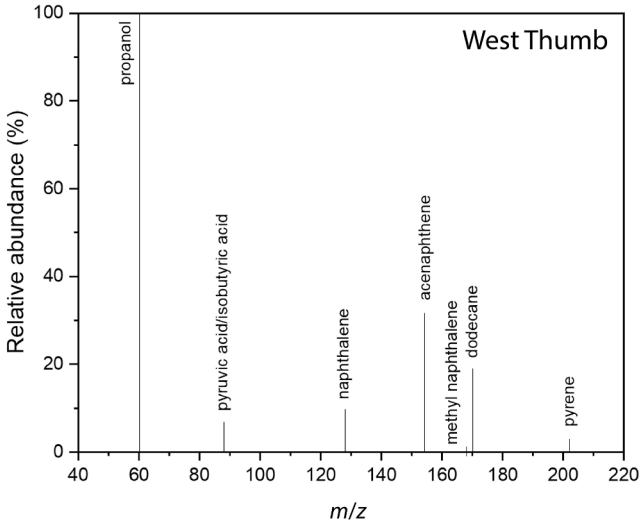

Fig. 3. Mass spectra with overlain peaks obtained by full scan mode showing major organic compounds identified in West Thumb vent fluids. Combined together, propanol (58.8%), the only alcohol present, is the most abundant compound, followed by PAHs (24.1%), alkanes (10.5%), and carboxylic acids (6.6%).

in Yellowstone (Schouten et al., 2007; Gonsior et al., 2018).

3.2.4. Order of abundance

The observed organic compounds have shown different proportions in SI Deep Hole and West Thumb. Even within each organic group, the relative order of abundance also varies.

3.2.4.1. Carboxylic acids. In SI Deep Hole, the relative order of abundance (Fig. 2) is: decanoic acid > malic acid > isobutyric/pyruvic acid > acetoacetic acid.

In West Thumb, other than pyruvic acid, isobutyric acid is also a major component of identified carboxylic acids. However, the relative abundance of both acids is the lowest among all compounds (Fig. 3).

3.2.4.2. PAHs. In SI Deep Hole, PAHs with simple structures have higher abundances than the ones with complex benzene ring structures. For example, naphthalene is present in most vent fluid samples, whereas pyrene was only observed in one sample with a very low concentration. The overall abundance shows the following order (Fig. 2): naphthalene > acenaphthene > methyl naphthalene > pyrene. In West Thumb, there is a change in the abundance of each PAH (Fig. 3). Acenaphthene becomes the most abundant PAH, with the order being: acenaphthene > naphthalene > pyrene > methyl naphthalene.

3.2.4.3. Cyclic hydrocarbons. The organic compounds consisting of cyclic structure are only identified in the YL16 series samples in SI Deep Hole. Collectively, cycloheptene is the most abundant organic compound in SI Deep Hole (Fig. 2).

3.2.4.4. Alcohols. Propanol is present in vent fluids from both locations, with the highest abundance of all organic compounds in West Thumb (Fig. 3). It was the only alcohol identified, and present in one sample. In addition, an alkane, dodecane in particular, was also identified. It exists in only one vent fluid sample from West Thumb. It has a higher overall abundance than carboxylic acids (Fig. 3). Altogether, in SI Deep Hole vent fluids, cyclic hydrocarbons have the highest abundance (43.3%), followed by carboxylic acids (36.6%), PAHs (19.3%), and alcohols (0.8%). At West Thumb, however, vent fluids reveal a different sequence, with alcohols (58.8%) being the most abundant species, followed by PAHs (24.1%), alkanes (10.5%), and carboxylic acids (6.6%).

Table 6
Carbon isotopic compositions* of dissolved CO_2 and CH_4 in samples collected from SI Deep Hole and West Thumb hydrothermal vents, with lake floor samples for comparison.

Sample	Isotopic composition (‰)	
	$\delta^{13}C_{CO2}$	$\delta^{13}C_{CH4}$
SI Deep Hole		
YL16F01	−9.9	−34.7
YL16F03	−10.3	−27.8
YL16F05	−9.5	−29.6
YL16F06	−7.5	−33.3
YL16F07	−6.4	−60.5
YL16F08	−9.2	−26.1
YL16F10	−10.2	−61.4
YL16F12	−10.5	−61.0
YL16F13	−9.4	−23.9
YL16F14	−8.9	−29.1
YL17F01	−5.8	−34.7
YL17F02	−5.8	−34.5
YL17F03	−4.7	−38.0
YL17F08	b.d.	−20.4
YL17F10	−4.4	−23.7
West Thumb		
YL18F11	−9.6	−19.0
YL18F14	−10.6	b.d.
YL18F15	−7.5	b.d.
YL18F17	−11.9	b.d.
YL18F19	−12.7	b.d.
Bottom Lake Water		
BLW2	−9.1	−32.1
BLW3	−10.9	−58.8

b.d.: below detection limit.
*The analytical error (1σ) for CO_2 is ± 0.5‰, while it varies from ± < 2‰ to 5‰ for CH_4, due to the low abundance of CH_4 and use of N_2 in sample collection and storage (see Section 2).

3.3. Carbon isotopes of dissolved CO_2 and CH_4

In SI Deep Hole vent fluids, the carbon isotopic composition of dissolved CO_2 ranges from −10.5‰ to −4.4‰ (Table 6). There is a temporal variation of carbon isotope values for CO_2 between the YL16 and YL17 samples. The $\delta^{13}C$ value of CO_2 ranges from −10.5‰ to −6.4‰ in the YL16 series, with the average being −9.2‰. The range becomes −5.8‰ to −4.4‰ in the YL17 samples, and the average reaches −5.2‰. The differences in carbon isotope compositions of CO_2 between YL16 and YL17 series are higher than the analytical uncertainties and may reflect real time-series changes.

Carbon isotope measurements have confirmed the presence of CH_4 at low concentrations, most of which are less than 0.22 mmol/kg (Fowler et al., 2019a). The carbon isotope values of CH_4 in the YL16 samples have two distinct ranges: −61.4‰ to −60.5‰ for 3 samples (YL16F07, YL16F10, and YL16F12), and −34.7‰ to −23.9‰ with the average of −29.2‰ for the rest. For the YL17 samples, the $\delta^{13}C$ value of CH_4 varies from −38.0‰ to −20.4‰, and the average is −30.3‰.

In West Thumb, the range of $\delta^{13}C$ values of CO_2 is between −12.7‰ and −7.5‰, with the average being −10.5‰. Only in one sample was CH_4 identified and analyzed for carbon isotopes, confirming the overall low abundance of CH_4 in vent fluids. Its $\delta^{13}C$ value is −19.0‰.

For the BLW samples, the carbon isotope values of CO_2 are −10.9‰ and −9.1‰, in a similar range as that observed in West Thumb and YL16 samples from SI Deep Hole. The $\delta^{13}C$ values of CH_4 are −58.8‰ and −32.1‰, with a striking difference between them, similar to the observation obtained from the YL16 samples from SI Deep Hole.

4. Discussion

4.1. Speciation and concentration of organic compounds

The vent fluids from SI Deep Hole and West Thumb have shown more diverse groups, elevated abundances, and complex structures of organic molecules than anticipated from bottom lake water alone (Tables 3, 4a, 4b, 5; Figs. 2 and 3). Carboxylic acids, PAHs, cyclic hydrocarbons, and alcohols are common groups present in vent fluids, which then provide a source of these species for the broader Yellowstone Lake system.

Combining all the organic carbon contents in vent fluid samples at each location together, the concentration of each organic group can be estimated as follows: In SI Deep Hole, cyclic hydrocarbons (2.5 mg/L), carboxylic acids (2.1 mg/L), PAHs (1.1 mg/L), and alcohols (0.1 mg/L); In West Thumb, alcohols (6.3 mg/L), PAHs (2.6 mg/L), alkanes (1.1 mg/L), and carboxylic acids (0.7 mg/L) (Table 7).

Organic compounds containing aliphatic and aromatic structures were reported in four subaerial hot springs in Yellowstone Park, including Narrow Gauge Spring, Rabbit Creek, Elk Geyser, and Octopus Spring (Gonsior et al., 2018). Most aliphatic compounds consist of $C_{3–5}$ branched, open-chains with methyl and carboxylic groups. Indeed, identical structures, carboxylic acids with $C_{3–4}$ chains (i.e., pyruvic, isobutyric, acetoacetic and malic acids), were identified in SI Deep Hole and West Thumb vent fluids (Tables 4a, 4b and 5).

4.2. Formation processes of organic compounds

4.2.1. Hydrothermal alteration/decomposition

The organic compounds in vent fluids from both sites are derived from organic precursors in subsurface rocks or sediments, that have been subject to alteration and/or decomposition from interactions with hydrothermal fluids. For example, previous studies have shown that short-chain carboxylic acids ($C_{3–5}$) are the predominant components formed during early diagenesis in petroliferous basins (Lewan and Fisher, 1994). The concentration of dissolved organic acids in formation water varied with temperature, with the maximum being in the range of 80–140 °C in Cenozoic clastic reservoirs (Lundegard and Kharaka, 1994).

In this study, a connection can be made between the relative quantity and structural complexity of organic groups in the vent fluids and geological conditions with hydrothermal processes involved. In SI Deep Hole vent fluids, the predominant occurrence of complex cyclic and unsaturated hydrocarbons, carboxylic acids, and PAHs may be attributed to the vapor-dominated hydrothermal system and corresponding heat and mass transport processes. This relationship is not only

Table 7
Estimated proportion and concentration of major organic groups identified in vent fluids from SI Deep Hole and West Thumb.

Organic Group	SI Deep Hole		West Thumb	
	Proportion (%)	Concentration (mg/L)	Proportion (%)	Concentration (mg/L)
Carboxylic acids	36.6	2.1	6.6	0.7
PAHs	19.3	1.1	24.1	2.6
Cyclic Hydrocarbons	43.3	2.5	n.d.	–
Alcohols	0.8	0.1	58.8	6.3
Alkanes	-*	–	10.5	1.1

* The percentage of alkanes in SI Deep Hole is too low to report.
n.d.: No detection of cyclic hydrocarbons in samples from West Thumb.

exhibited in the hydrothermal upflow zone where lake water is entrained and temperature is above 100 °C, but also present at depths where boiling fluids containing gases (CO_2, H_2S, and H_2) flow through fractures with a significant amount of heat (Fowler et al., 2019a,b; Tan et al., 2020). In addition to high temperature water, the extraction of organic compounds from rocks or sediments is enhanced in the presence of H_2 which works as a chain breaker (Lewan, 1997; Lewan and Roy, 2011), and supercritical CO_2 under elevated pressures (Monin et al., 1988; Greibrokk et al., 1992). Combined with the lack of primary diatomaceous lake floor sediments and vent lithology characterized by kaolinite and boehmite due to intensive hydrothermal alteration (Shanks et al., 2005, 2007; Fowler et al., 2019a,b), the results suggest a dominantly deep and/or distant source of organic components in vent fluids in SI Deep Hole.

In contrast, the geological conditions and fluid-rock interactions are different in West Thumb. There are abundant siliceous structures and hydrothermally silicified sediments surrounding vent areas, showing alteration features to a lesser extent than in SI Deep Hole (Fowler et al., 2019a). The fluids are enriched in Cl^- with neutral pH values, similar to many hydrothermal fluids from subaerial geysers in Yellowstone. The measured sample temperatures are in the range of 36–80 °C, with only one above 100 °C (Table 1). All of those physical and chemical conditions contribute to the presence of simple and light organic molecules in vent fluids, including propanol and *n*-dodecane, through alteration/decomposition of organic matter in lake sediments or basement rocks.

Previous studies have also shown the control of hydrothermal processes (geological conditions, fluid chemistry, etc.) on generated hydrocarbons. Vent fluids from Middle Valley (Dead Dog and ODP Mound fields) and Main Endeavor field (MEF), which are approximately 70 km apart on the northern Juan de Fuca Ridge, northeast Pacific, were analyzed for organic compositions (Cruse and Seewald, 2006, 2010). In the sediment-covered Middle Valley, light organic molecules, including alkanes (C_1–C_4), alkenes (C_2–C_3), and aromatic hydrocarbons (benzene and toluene), are present in fluids from both Dead Dog and ODP Mound fields. They are generated from organic matter in subsurface regions that have undergone alteration with hydrothermal fluids, whereas methane may also be the product of bacterial activity during seawater circulation (Cruse and Seewald, 2006). The concentrations of those light organic compounds in Dead Dog field, however, are higher than in ODP Mound. This is caused by the difference in subsurface environment and corresponding hydrothermal processes. The estimated subsurface temperature in Dead Dog is 350 °C, while the maximum temperature in ODP Mound is 420 °C which implies a separated vapor phase for hydrothermal fluids. The stepwise oxidation reactions of alkanes with H_2O at higher temperatures are responsible for their lower abundances in ODP Mound field (Seewald, 2001; Cruse and Seewald, 2006). A similar suite of organic compounds was also identified in vent fluids from MEF, a well-developed sediment-free axial rift valley associated with the Juan de Fuca Ridge (Cruse and Seewald, 2010). It has been suggested that the sediments buried at an earlier stage of the ridge's evolution (Lilley et al., 1993) or the sediments at Middle Valley may be the source of organics (Cruse and Seewald, 2010). The chemical redox condition at MEF or longer residence time of fluids during circulation promotes a different abundance and distribution pattern of organic compounds than at Middle Valley (Cruse and Seewald, 2010).

A diverse spectrum of dissolved organic content was identified in vent fluids from back-arc basins in southwest Pacific: Kulo Lasi and Fatu Kapa vent fields (Konn et al., 2018). The organic compounds consist of *n*-alkanes (C_9–C_{12}), fatty acids (C_9, C_{12}, C_{14}–C_{18}), and PAHs (fluorene, phenanthrene, and pyrene), with variation in concentration at the part-per-billion (μmol/kg) level and different distribution patterns of organic groups. The fluid chemistry suggests high temperature (338–343 °C) fluids with a separated gas phase at Kulo Lasi, and typical hydrothermal fluids derived from interaction of seawater with basalt and felsic lava at Fatu Kapa. Lines of evidence have shown that both biological activity and thermal decomposition of organic matter make significant contribution to the generation of dissolved organic molecules (Konn et al., 2018). The combination of those processes may not be limited to subseafloor hydrothermal systems in different tectonic settings (mid-ocean ridges, back-arc basins, etc.). A similar set of reactions can occur in continental hydrothermal systems, as observed in Yellowstone Lake in the present study.

In summary, organic compounds in vent fluids from both sites in Yellowstone Lake are mainly generated from the interactions between hydrothermal fluids and subsurface organic precursors. Compared to subseafloor hydrothermal systems, the diversity of organic compositions and abundances observed here is the reflection of geological conditions (temperature in particular) and fluid chemistry (separated gas phases, redox, dissolved H_2 content, etc.). The chemical composition of the organic precursors may also contribute to this diversity. For example, elemental compositions and microconstituents (i.e., macerals) are different for kerogen in terrestrial and marine sediments (Alpern,1980; Durand and Monin, 1980). Without further analysis, however, the evaluation of the role of organic precursors in vent fluid compositions is inconclusive.

4.2.2. PAHs

Among the complex organic compounds present in vent fluids, the concentration of PAHs in West Thumb (2.6 mg/L) is more than two times higher than the value (1.1 mg/L) in SI Deep Hole (Table 7). The PAHs account for approximately 24.1% of the total organic compounds in West Thumb. Similarly, more diverse PAHs and cyclic hydrocarbons were identified in dredge samples in Guaymas Basin (Simoneit and Lonsdale, 1982; Simoneit, 1983). Such complex organic compounds may be generated together with simple molecules (alcohols, alkanes, etc.) through fluid-rock interactions. In West Thumb, those interactions take place either in the upflow zone where alteration of minerals proceeds simultaneously, or in the deep subsurface where high temperature fluids circulate and mix with meteoric water before ascending to the lake floor.

Indeed, the total amount of PAHs and organic carbon in lake bed sediments was measured at the outlet of the lake at the Yellowstone River (Peterson and Boughton, 1998). The study reported a TOC value of 6.9 g/kg sediment, while the amount of PAHs was 18 μg/kg sediment with their proportion being 2.6 μg/g organic carbon. It may be

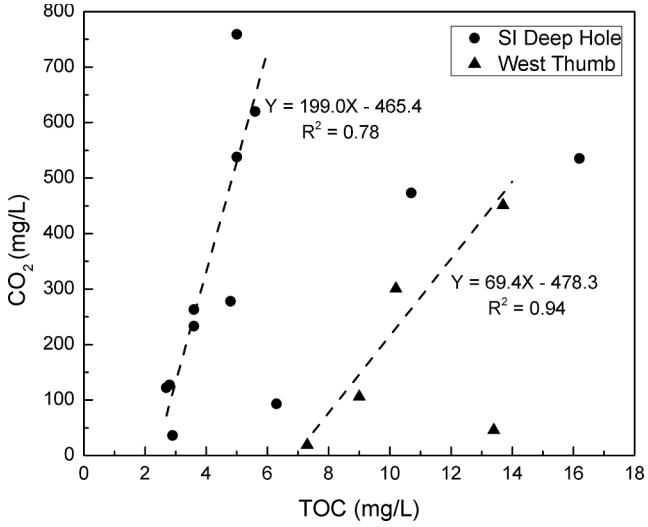

Fig. 4. The TOC value and dissolved CO_2 concentration in vent fluids from SI Deep Hole and West Thumb. A positive correlation (dash line) can be observed in most samples from each hydrothermal system (i.e., 9 of 12 samples for SI Deep Hole, and 4 of 5 samples for West Thumb). However, this relationship never implies dissolved organic compounds and CO_2 in vent fluids share the same source (see Section 4.2.3).

unreasonable or even impossible to compare the PAH content in sediments and vent fluids, due to constant interactions between them. However, these data suggest the widespread presence of PAHs in sediments sourced from the Yellowstone Lake, although the low percentage at the 10^{-6} level was present in sedimentary organics farther away from hydrothermal vents.

4.2.3. TOC

Similar to the trend observed in PAHs, the average TOC value of vent fluids from SI Deep Hole, 4.0 mg/L (YL16 samples) and 9.2 mg/L (YL17 samples), is less than 10.7 mg/L, the average for fluids from West Thumb (Table 2). As described above, the lack of organic-bearing sediments on the lake floor and shallow subsurface, due to extensive hydrothermal alteration at SI Deep Hole, may also be responsible for lower levels of TOC in SI Deep Hole fluids. Furthermore, the alteration of organic compounds is enhanced to a greater extent by high-temperature fluids having a vapor phase.

It is worth noting that there is a positive correlation between TOC and dissolved CO_2 concentration in vent fluids from each hydrothermal system (Fig. 4). The regression functions, Eqs. (1) and (2), show linear relationship for most samples (9 of 12 samples for SI Deep Hole, 4 of 5 samples for West Thumb):

$$\text{SI Deep Hole}: \text{Dissolved } CO_2\ (\text{mg/L}) = 199.0 \times \text{TOC}\ (\text{mg/L}) - 465.4 \quad (1)$$

$$\text{West Thumb}: \text{Dissolved } CO_2\ (\text{mg/L}) = 69.4 \times \text{TOC}\ (\text{mg/L}) - 478.3 \quad (2)$$

The coefficient of determination (R^2) is 0.78 and 0.94 for Eqs. (1) and (2), respectively. This positive correlation suggests there is a connection between the amount of TOC and the presence of CO_2, both of which are ultimately related to heat and mass transfer during emplacement of magma. However, it never implies that the dissolved CO_2 shares the same source as organic compounds in vent fluids (see discussion in Section 4.3.2).

A number of fluid samples were collected for measurement of dissolved organic carbon from hydrothermal vents on the Juan de Fuca Ridge (Lang et al., 2006). Those vent fields include two young unsedimented axial sites (MEF and Axial Volcano) and two off-axis flank sites (Baby Bare Seamount and ODP Hole 1026B). Both axial sites contain high temperature (212–374 °C) and diffuse (up to 85 °C) venting. The results have shown that high-temperature vent fluids sampled at MEF and Axial Volcano (15 ± 5 and 17 ± 8 μM, respectively) are depleted in organic carbon compared to low-temperature diffuse fluids (49 ± 9 μM and 50 ± 10 μM, respectively) in the same area. The concentrations of organic carbon in fluids from older, low-temperature ridge-flank sites, Baby Bare Seamount (20 °C) and ODP Hole 1026B (63 °C), are similar (10 ± 3 μM and 13 ± 4 μM, respectively) and far less than the level (36 μM) present in the source water (North Pacific Deep Water; Lang et al., 2006). These results suggest that the variation of total organic carbon concentrations in fluids from different vent sites may be attributed to a number of processes, including microbial consumption and production at lower temperatures, adsorption to and desorption from mineral surfaces, and thermal decomposition of organic matter.

Altogether, the observed difference in organic speciation and concentration in SI Deep Hole and West Thumb vent fluids in Yellowstone Lake is a manifestation of interactions between hydrothermal fluids and sediments or subsurface rocks, underscoring further the essential role of environmental conditions and fluid chemistry in generation of organic compounds in both subseafloor and continental hydrothermal systems.

4.3. Carbon isotope signatures

4.3.1. Methane (CH_4)

Methane in hydrothermal systems can be derived from a variety of carbon sources, by different processes, and under a wide range of chemical and physical conditions. The principal sources of methane in hydrothermal fluids include: “thermogenic” – cracking and decomposition of complex organic matter at elevated temperatures; “biogenic” – fermentation and CO_2 reduction by bacteria at low temperatures; and “abiogenic” – outgassing of juvenile carbon from the mantle (in significantly lower amounts), or inorganic synthesis at high temperatures involving CO_2 and H_2 or other C-H molecules which may be derived from various sources (Des Marais et al., 1981; Schoell, 1988; Welhan, 1988; Whiticar, 1990; Kelley, 1996; Kelley and Früh-Green, 1999; Sherwood Lollar et al., 2002, 2006; Fiebig et al., 2009; Wang et al., 2015, 2018).

The carbon isotopic composition of methane has been used as a diagnostic tool for identifying its origin. The $\delta^{13}C$ value of methane derived thermocatalytically from organic matter is generally lower than −25‰ (V-PDB), while low-temperature bacteria-produced methane is much more depleted in ^{13}C with values less than −60‰ (Schoell, 1983; Lyon and Hulston, 1984; Schoell, 1988; Welhan, 1988; Whiticar, 1990; Giggenbach, 1997). For distinguishing methane of abiogenic origin, one suggested criteria is $\delta^{13}C$ values higher than −25‰, based on limited isotopic data of abiogenic methane (Jenden et al., 1993). For example, methane generated in sedimentary basins that are associated with oil and natural gases has shown a large isotopic variation between −60‰ and −25‰, depending on multiple processes before and after its formation including sedimentation, maturation, expulsion, and accumulation (Schoell, 1988; Liu et al., 2019). Moreover, the $\delta^{13}C$ value of methane is also constrained by kinetic processes while approaching full equilibrium with other gases (CO_2 in particular), dissolved carbon species, or organic carbon source in hydrothermal systems with high heat flow (>80 mW/m^2) (Giggenbach, 1997). Using the above criteria alone is insufficient to identify the origin of methane. For example, experimental studies have shown that production of abiogenic methane under conditions encountered in subseafloor serpentinization reactions results in very low $\delta^{13}C$ values, which may overlap values typical for bacterial methane (Horita and Berndt, 1999).

The samples from SI Deep Hole have $\delta^{13}C$ values in the range of −34.7‰ to −23.9‰, except for three samples with values less than

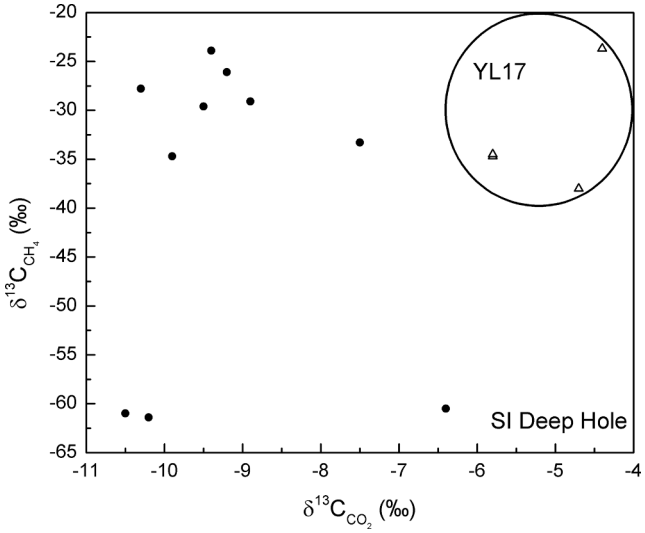

Fig. 5. The $\delta^{13}C$ values of dissolved CO_2 and CH_4 in vent fluids from SI Deep Hole. The dominant source of CH_4 is organic matter in subsurface rocks and lake sediments that have been subject to hydrothermal alteration/decomposition. Microbial activities on the lake floor may also contribute to CH_4 formation. Magmatic degassing is the major source of CO_2, whereas lower amounts of CO_2 are generated accompanying CH_4 and other organic compounds through thermogenic processes. The temporal enrichment in ^{13}C for CO_2 in YL17 samples may be caused by the input of higher amounts of CO_2 from underlying magmatic bodies.

−60‰ (Table 6, Fig. 5). These data suggest that the dominant source of methane is thermogenic processes applied to subsurface rocks or lake sediments, through which other dissolved organic compounds may also be generated. The depletion of ^{13}C in three samples may indicate microbial activities on the lake floor, which is corroborated by the depleted $\delta^{13}C$ value of −58.8‰ from one BLW sample. Due to the low methane concentration and analytical uncertainty (± < 2‰ to 5‰) involving dilution with N_2 during sample collection, the only $\delta^{13}C$ value obtained from West Thumb, −19.0‰, suggests similar geothermal (thermogenic) processes, supporting the conclusions of previous studies (Des Marais et al., 1981; Lorenson et al., 1991; Bergfeld et al., 2011).

Carbon isotope measurements of methane from several subaerial geothermal springs in Yellowstone were carried out by Moran et al. (2017). The $\delta^{13}C$ value varied between −20.5‰ and −30.2‰, similar to the range observed in our study. It was suggested that in addition to a thermogenic source, abiotic reduction of magmatic CO_2 is the predominant process of methane generation, supported by the isotopic equilibrium between methane and dissolved inorganic carbon in fluids. In our study, lines of evidence in subsurface geological conditions and $\delta^{13}C$ values of CO_2 point to a primarily thermogenic origin of methane in SI Deep Hole and West Thumb vent fluids (see more discussion in Section 4.3.2), confirming again the effect of environmental conditions on the generation of organic compounds, which may have multiple sources and formation processes in Yellowstone.

4.3.2. Carbon dioxide (CO_2)

The carbon isotope value of CO_2 in the SI Deep Hole vent fluids varies from −10.5‰ to −4.4‰ (Table 6, Fig. 5). There is a temporal enrichment of ^{13}C for the YL17 samples, with the average $\delta^{13}C$ value increasing from −9.2‰ (YL16) to −5.2‰ (YL17). A similar range, −12.7‰ to −7.5‰, is observed for samples from West Thumb (Table 6). Together, most samples are depleted in ^{13}C compared to the range of −5‰ to −1‰ obtained from a number of subaerial fumaroles and hot springs (Craig, 1963; Kharaka et al., 1992; Werner and Brantley, 2003).

There is no attainment of isotopic equilibrium between dissolved CH_4 and CO_2 at sampling temperatures (Fig. 6), using the fractionation factors from Horita (2001):

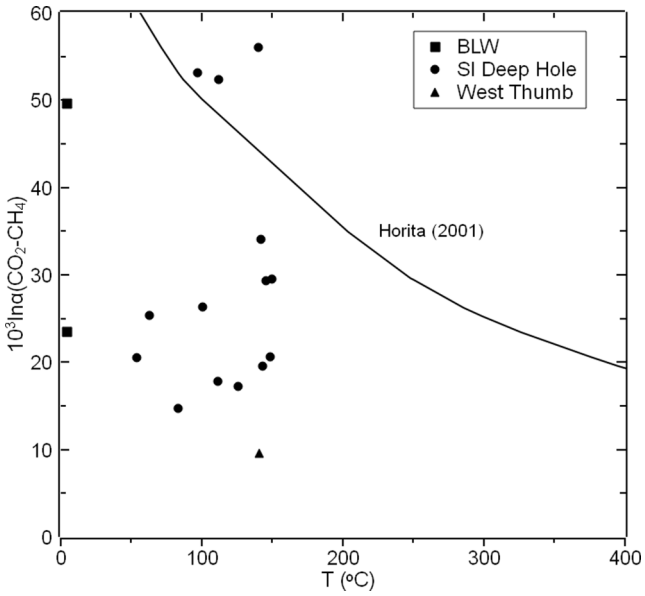

Fig. 6. The difference in $\delta^{13}C$ values ($10^3 \ln\alpha$) between CO_2 and CH_4 with measured sampling temperature for vent fluids from SI Deep Hole and West Thumb. The average temperature value was used if temperature varied while sampling (Table 1). No isotopic equilibrium is attained between dissolved CH_4 and CO_2 at sampling temperatures, using the fractionation factors from Horita (2001). The sampling temperatures are lower than the predicted equilibrium temperatures for most samples, while the opposite is true for three samples from SI Deep Hole containing microbial methane. The discrepancy between sampling and predicted temperatures suggests CH_4 and CO_2 may have different origins (see Section 4.3.2).

$$10^3 \ln\alpha(CO_2 - CH_4) = 0.16 + 11.754\left(10^6/T^2\right) - 2.3655\left(10^9/T^3\right) + 0.2054\left(10^{12}/T^4\right) \quad (3)$$

For most samples from SI Deep Hole and the only sample available from West Thumb, the sampling temperatures are lower than the temperatures predicted by the above carbon isotope geothermometer (Eq. (3)), which are in the range of 204–516 °C (SI Deep Hole) and 740 °C (West Thumb) (Fig. 6). The opposite is true for the three samples that contain microbial methane, showing higher sampling temperatures than predicted (71–87 °C). Similar observations were reported for fluids from a number of continental geothermal fields and mid-ocean ridge hydrothermal systems (Panichi et al., 1977; Nuti et al., 1980; Lyon and Hulston, 1984; Evans et al., 1988; Welhan, 1988; Podera et al., 1992; Giggenbach, 1997; Kelley and Früh-Green, 1999). A majority of the predicted equilibrium temperatures using the carbon isotope geothermometer (Eq. (3)) are higher than the maximum temperature of the vent fluids at subsurface in both fields (Fowler et al., 2019a,b), and the temperature (360 °C) of the perceived common hydrothermal reservoir shared by hydrothermal waters in Yellowstone (Hurwitz and Lowenstern, 2014). It implies that no isotopic equilibrium between CH_4 and CO_2 is attained under subsurface conditions, and the reduction of CO_2 is not the predominant process for methane generation. The discrepancy between sampling and predicted temperatures suggests that CH_4 and CO_2 may have different origins and have never reached isotopic equilibrium. Alternatively, the addition of CH_4 or CO_2 of a different origin to ascending fluids may cause deviation from the isotopic equilibrium that may have been previously attained at subsurface. Nevertheless, either interpretation would imply CO_2 has a different origin than CH_4 in vent fluids.

Prior studies have shown that the source of CO_2 in YPVF may include magmatic degassing, thermal breakdown of organic matter in sediments, and hydrolysis of carbonates at depths (Werner and Brantley, 2003). The measured $\delta^{13}C$ value of CO_2 from fumaroles at Yellowstone is consistent with the range for CO_2 with a basaltic magma source (Craig, 1963; Werner and Brantley, 2003). Recent fluid chemistry results suggest saturation of CO_2 under subsurface temperature and pressure conditions at SI Deep Hole (Fowler et al., 2019a,b; Tan et al., 2020). Thus, the predominant source of CO_2 is most likely to be magmatic degassing. Thermal decomposition of organic matter also generates CO_2, as commonly observed during petroleum generation in sedimentary basins, but in lower amounts. The contribution from each individual source is hard to quantify definitively, owing to the lack of constraints on carbon isotope values of mantle CO_2 and organic matter in this area. The temporal ^{13}C enrichment of the average from −9.2‰ (YL16) to −5.2‰ (YL17) in SI Deep Hole suggests higher amount of CO_2 input from underlying magmatic bodies (Fig. 5). The correspondingly enhanced heat transfer contributes to the elevated TOC values of the YL17 samples.

5. Conclusions

The first characterization of organic compounds in sublacustrine vent fluids from SI Deep Hole and West Thumb on the floor of Yellowstone Lake has confirmed the existence of diverse functional groups and molecular structures: cyclic hydrocarbons, carboxylic acids, PAHs, alcohols, and alkanes. The generation and distribution of these compounds may be controlled by the local temperature regime, which is manifested at the SI Deep Hole by vapor-dominated hydrothermal alteration processes and a hot water vent system at West Thumb. The uniquely different heat and mass transport processes at each of the vent systems undoubtedly contribute to the observed organic geochemistry, as they do to the alteration mineralogy and physical characteristics of the hydrothermal upflow zones and extent and location of lake water mixing effects. There are multiple sources for dissolved organic species. A thermogenic origin is dominant, with organic matter in subsurface rocks and lake sediments serving as the precursor. In addition, microbial activities on the lake floor may contribute to methane formation. Magmatic degassing is the major process responsible for dissolved CO_2.

The observations made in this study have illustrated the interplay of geological (magma degassing), chemical (thermal decomposition of organic matter), and biological (microbial methane formation) processes in Yellowstone Lake, and their imprints on vent fluids. Indeed, the connection between vapor-dominated hydrothermal alteration, elevated TOC contents and dissolved CO_2 in vent fluids, and enrichment of ^{13}C in CO_2 in YL17 samples in SI Deep Hole manifest best this close association. Altogether, they are integral parts of the carbon cycle in the Yellowstone Lake ecosystem.

Declaration of Competing Interest

The authors declare that they have no known competing financial interests or personal relationships that could have appeared to influence the work reported in this paper.

Acknowledgements

Funding support from NSF grants EAR-1515377 and OCE-1434798 to WES, and NSF CAREER program under award OCE-1652481 to QF are acknowledged. All work in Yellowstone National Park was completed under an authorized Yellowstone research permit (YELL-2018-SCI-7018). We would like to thank two anonymous reviewers for their comments and suggestions, which improved the manuscript significantly. Helpful comments by the Associate Editor Kliti Grice and Co-Editor-in-Chief John Volkman are also appreciated.

References

Alpern, B., 1980. Pétrographie du kérogène. In: Durand, B. (Ed.), Kerogen: Insoluble Organic Matter from Sedimentary Rocks. Editions Technip, Paris, pp. 339–383.

Balistrieri, L.S., Shanks III, W.C.P., Cuhel, R.L., Aguilar, C., Klump, J.V., 2007. The influence of sublacustrine hydrothermal vent fluids on the geochemistry of Yellowstone Lake. In: Morgan, L.A. (Ed.), Integrated Geoscience Studies in the Greater Yellowstone Area- Volcanic, Tectonic, and Hydrothermal Processes in the Yellowstone Geoecosystem. U.S. Geological Survey Professional Paper 1717, pp. 173–197.

Barns, S.M., Fundyga, R.E., Jeffries, M.W., Pace, N.R., 1994. Remarkable archaeal diversity detected in a Yellowstone National Park hot spring environment. Proc. Natl. Acad. Sci. USA 91, 1609–1613.

Bergfeld, D., Lowenstern, J.B., Hunt, A.G., Shanks III, W.C.P., Evans, W.C., 2011. Gas and isotope chemistry of thermal features in Yellowstone National Park, Wyoming. U.S. Geological Survey Scientific Investigation Report 2011-5012, pp. 1–26.

Christiansen, R.L., 1984. Yellowstone magmatic evolution: Its bearing on understanding large-volume explosive volcanism. In: Explosive Volcanism: Inception, Evolution, and Hazards. Studies in Geophysics. National Academy Press, Washington, pp. 84–95.

Christiansen, R.L., 2001. The Quaternary and Pliocene Yellowstone Plateau Volcanic Field of Wyoming, Idaho, and Montana. U.S. Geological Survey Professional Paper 729-G, pp. 1–145.

Christiansen, R.L., Blank Jr., H.R., 1972. Volcanic stratigraphy of the Quaternary rhyolite plateau in Yellowstone National Park. U.S. Geological Survey Professional Paper 729-B, pp. 1–18.

Clifton, C.G., Walters, C.C., Simoneit, B.R.T., 1990. Hydrothermal petroleums from Yellowstone National Park, Wyoming, U.S.A. Appl. Geochem. 5, 169–191.

Clingenpeel, S., Macur, R.E., Kan, J., Inskeep, W.P., Lovalvo, D., Varley, J., Mathur, E., Nealson, K., Gorby, Y., Jiang, H., LaFracois, T., McDermott, T.R., 2011. Yellowstone Lake: high-energy geochemistry and rich bacterial diversity. Environ. Microbiol. 13, 2172–2185.

Craig, H., 1963. The isotopic geochemistry of water and carbon in geothermal areas, In: Tongiorgo, E. (Ed.), Proceedings of the Conference on Nuclear Geology in Geothermal Areas, Spoleto 1963. Lishchi, Pisa, Italy.

Cruse, A.M., Seewald, J.S., 2006. Geochemistry of low molecular weight hydrocarbons in hydrothermal fluids from Middle Valley, northern Juan de Fuca Ridge. Geochim. Cosmochim. Acta 70, 2073–2092.

Cruse, A.M., Seewald, J.S., 2010. Low-molecular weight hydrocarbons in vent fluids from Main Endeavour Field, northern Juan de Fuca Ridge. Geochim. Cosmochim. Acta 74, 6126–6140.

Des Marais, D.J., Donchin, J.H., Nehring, M.L., Truesdell, A.H., 1981. Molecular carbon isotopic evidence for the origin of geothermal hydrocarbons. Nature 292, 826–828.

Durand, B., Monin, J.C., 1980. Elemental analysis of kerogens. In: Durand, B. (Ed.), Kerogen: Insoluble Organic Matter from Sedimentary Rocks. Editions Technip, Paris, pp. 113–142.

Evans, W.C., White, L.D., Rapp, J.B., 1988. Geochemistry of some gases in hydrothermal fluids from the southern Juan de Fuca Ridge. J. Geophys. Res. 93, 15305–15313.

Fiebig, J., Woodland, A.B., D'Alessandro, W., Püttmann, W., 2009. Excess methane in continental hydrothermal emissions is abiogenic. Geology 37, 495–498.

Fournier, R.O., 1989. Geochemistry and dynamics of the Yellowstone National Park hydrothermal system. Annu. Rev. Earth Planet. Sci. 17, 13–53.

Fowler, A.P.G., Tan, C., Luttrell, K., Tudor, A., Scheuermann, P., Shanks III, W.C.P., Seyfried Jr., W.E., 2019. Geochemical heterogeneity of sublacustrine hydrothermal vents in Yellowstone Lake, Wyoming. J. Volcanol. Geotherm. Res. 386, 106677.

Fowler, A.P.G., Tan, C., Cino, C.D., Scheuermann, P., Volk, M.W.R., Shanks III, W.C.P., Seyfried Jr., W.E., 2019. Vapor-driven sublacustrine vents in Yellowstone Lake, Wyoming, USA. Geology 47, 223–226.

Fowler, A.P.G., Liu, Q.-L., Huang, Y., Tan, C., Volk, M.W.R., Shanks III, W.C.P., Seyfried Jr., W.E., 2019. Pyrite $\delta^{34}S$ and $\Delta^{33}S$ constraints on sulfur cycling at sublacustrine hydrothermal vents in Yellowstone Lake, Wyoming, USA. Geochimica et Cosmochimica Acta 265, 148–162.

Fritz, W.J., 1985. Roadside Geology of the Yellowstone Country. Mountain Press Publishing Company, Montana, USA.

Gemery-Hill, P.A., Shanks III, W.C., Balistrieri, L.S., Lee, G.K., 2007. Geochemical data for selected rivers, lake waters, hydrothermal vents, and subaerial geysers in Yellowstone National Park, Wyoming and Vicinity, 1996-2004. In: Morgan, L.A. (Ed.), Integrated Geoscience Studies in the Greater Yellowstone Area-Volcanic, Tectonic, and Hydrothermal Processes in the Yellowstone Geoecosystem. U.S. Geological Survey Professional Paper 1717, pp. 365–426.

Giggenbach, W.F., 1997. Relative importance of thermodynamic and kinetic processes in governing the chemical and isotopic composition of carbon gases in high-heatflow sedimentary basins. Geochim. Cosmochim. Acta 61, 3763–3785.

Gonsior, M., Hertkorn, N., Hinman, N., Dvorski, S.E.M., Harir, M., Cooper, W.J., Schmitt-Kopplin, P., 2018. Yellowstone hot springs are organic chemodiversity hot spots. Sci. Rep. 8, 1–12.

Greibrokk, T., Radke, M., Skurdal, M., Willsch, H., 1992. Multistage supercritical fluid extraction of petroleum source rocks: application to samples from Kimmeridge clay and Posidonia Shale formations. Org Geochem. 18, 447–455.

Hawkes, J.A., Rossel, P.E., Stubbins, A., Butterfield, D., Connelly, D.P., Achterberg, E.P., Koschinsky, A., Chavagnac, V., Hansen, C.T., Bach, W., Dittmar, T., 2015. Efficient removal of recalcitrant deep-ocean dissolved organic matter during hydrothermal circulation. Nat. Geosci. 8, 856–860.

Horita, J., 2001. Carbon isotope exchange in the system CO_2-CH_4 at elevated temperatures. Geochim. Cosmochim. Acta 65, 1907–1919.

Horita, J., Berndt, M.E., 1999. Abiogenic methane formation and isotopic fractionation under hydrothermal conditions. Science 285, 1055–1057.

Hurwitz, S., Lowenstern, J.B., 2014. Dynamics of the Yellowstone hydrothermal system. Rev. Geophys. 52, 375–411.

Inskeep, W.P., Ackerman, G.G., Taylor, W.P., Kozubal, M., Korf, S., Macur, R.E., 2005. On the energetics of chemolithotrophy in nonequilibrium systems: Case studies of geothermal springs in Yellowstone National Park. Geobiology 3, 297–317.

Inskeep, W.P., Jay, Z.J., Macur, R.E., Clingenpeel, S., Tenney, A., Lovalvo, D., Beam, J.P., Kozubal, M.A., Shanks, W.C., Morgan, L.A., Kan, J., Gorby, Y., Yooseph, S., Nealson, K., 2015. Geomicrobiology of sublacustrine thermal vents in Yellowstone Lake: geochemical controls on microbial community structure and function. Front. Microbiol. 6, 1044.

Jenden P.D., Hilton, D.R., Kaplan, I.R., Craig, H., 1993. Abiogenic hydrocarbons and mantle helium in oil and gas fields. In: Howell, D.G., Wiese, K., Fanelli, M., Zink, L. L., Cole, F. (Eds.), The Future of Energy Gases. U.S. Geological Survey Professional Paper 1570, pp. 31–56.

Kan, J., Clingenpeel, S.R., Macur, R., Inskeep, W.P., Lavalvo, D., Varley, J., Nealson, K., McDermott, T.R., 2011. Archaea in Yellowstone Lake. Multidiscip. J. Microb. Ecol. 5, 1784–1795.

Kelley, D.S., 1996. Methane-rich fluids in the oceanic crust. J. Geophys. Res. 101, 2943–2962.

Kelley, D.S., Früh-Green, G.L., 1999. Abiogenic methane in deep-seated mid-ocean ridge environments: insights from stable isotope analyses. J. Geophys. Res. Solid Earth 104, 10439–10460.

Kharaka, Y.K., Mariner, R.H., Evans, W.C., Kennedy, B.M., 1992. Composition of gases from the Norris-Mammoth corridor, Yellowstone National Park, U.S.A.: Evidence for magmatic source near Mammoth Hot Springs. In: Kharaka, Y.K., Maest K.A. (Eds.), Water-Rock Interaction. A. A. Balkema, Brookfield, Vermont, USA, pp. 1303–1307.

Klump, J.V., Remsen, C.C., Kaster, J.L., 1988. The presence and potential impact of geothermal activity on the chemistry and biology of Yellowstone Lake, Wyoming. In: De Luca, M.P., Babb, I. (Eds.), Global Venting, Midwater, and Benthic Ecological Processes. National Oceanic and Atmospheric Administration National Undersea Research Program Research Report 88-4, pp. 81–98.

Konn, C., Donval, J.P., Guyader, V., Roussel, E., Fourré, E., Jean-Baptiste, P., Pelleter, E., Charlou, J.L., Fouquet, Y., 2018. Organic, gas, and element geochemistry of hydrothermal fluids of the newly discovered extensive hydrothermal area in the Wallis and Futuna Region (SW Pacific). Geofluids 2018, 7692839.

Lang, S.Q., Butterfield, D.A., Lilley, M.D., Johnson, H.P., Hedges, J.I., 2006. Dissolved organic carbon in ridge-axis and ridge-flank hydrothermal systems. Geochim. Cosmochim. Acta 70, 3830–3842.

Lanphere, M.A., Champion, D.E., Christiansen, R.L., Izett, G.A., Obradovich, J.D., 2002. Revised ages for tuffs of the Yellowstone Plateau volcanic field: Assignment of the Huckleberry Ridge Tuff to a new geomagnetic polarity event. Geol. Soc. Am. Bull. 114, 559–568.

Lewan, M.D., 1997. Experiments on the role of water in petroleum formation. Geochim. Cosmochim. Acta 61, 3691–3723.

Lewan, M.D., Fisher, J.B., 1994. Organic acids from petroleum source rocks. In: Pittman, E.D., Lewan, M.D. (Eds.), Organic Acids in Geological Processes. Springer, Berlin Heidelberg, pp. 70–114.

Lewan, M.D., Roy, S., 2011. Role of water in hydrocarbon generation from Type-I kerogen in Mahogany oil shale of the Green River Formation. Org Geochem. 42, 31–41.

Lilley, M.D., Butterfield, D.A., Olson, E.J., Lupton, J.E., Macko, S.A., McDuff, R.E., 1993. Anomalous CH_4 and NH_4^+ concentrations at an unsedimented mid-ocean-ridge hydrothermal system. Nature 364, 45–47.

Liu, Q., Wu, X., Wang, X., Jin, Z., Zhu, D., Meng, Q., Huang, S., Liu, J., Fu, Q., 2019. Carbon and hydrogen isotopes of methane, ethane, and propane: A review of genetic identification of natural gas. Earth Sci. Rev. 190, 247–272.

Lorenson, T.D., Kvenvolden, K.A., Simoneit, B.R., Leif, R.N., 1991. Composition of gas seeps in northwestern Wyoming. U.S. Geological Survey Open File Report 91-121, pp. 1–35.

Lovalvo, D., Clingenpeel, S.R., Mcginnis, S., Macur, R.E., Varley, J.D., Inskeep, W.P., Glime, J., Nealson, K., McDermott, T.R., 2010. A geothermal-linked biological oasis in Yellowstone Lake, Yellowstone National Park, Wyoming. Geobiology 8, 327–336.

Lundegard, P., Kharaka, Y., 1994. Distribution and occurrence of organic acids in subsurface waters. In: Pittman, E.D., Lewan, M.D. (Eds.), Organic Acids in Geological Processes. Springer, Berlin Heidelberg, pp. 40–69.

Lyon, G.L., Hulston, J.R., 1984. Carbon and hydrogen isotopic compositions of New Zealand geothermal gases. Geochim. Cosmochim. Acta 48, 1161–1171.

Meyer-Dombard, D.R., Shock, E.L., Amend, J.P., 2005. Archaeal and bacterial communities in geochemically diverse hot springs of Yellowstone National Park, USA. Geobiology 3, 211–227.

Monin, J.C., Barth, D., Perrut, M., Espitalié, M., Durand, B., 1988. Extraction of hydrocarbons from sedimentary rocks by supercritical carbon dioxide. Org Geochem. 13, 1079–1086.

Moran, J.J., Whitmore, L.M., Jay, Z.J., Jennings, R.deM., Beam, J.P., Kreuzer, H.W., Inskeep, W.P., 2017. Dual stable isotopes of CH_4 from Yellowstone hot-springs suggest hydrothermal processes involving magmatic CO_2. J. Volcanol. Geotherm. Res. 341, 187–192.

Morgan, L.A., Shanks III, W.C., Lovalvo, D.A., Johnson, S.Y., Stephenson, W.J., Pierce, K. L., Harlan, S.S., Finn, C.A., Lee, G., Webring, M., Schulze, B., Dühn, J., Sweeney, R., Balistrieri, L., 2003. Exploration and discovery in Yellowstone Lake: results from high-resolution sonar imaging, seismic reflection profiling, and submersible studies. J. Volcanol. Geoth. Res. 122, 221–242.

Morgan, L.A., Shanks III, W.C., Pierce, K.L., Lovalvo, D.A., Lee, G.K., Webring, M.W., Stephenson, W.J., Johnson, S.Y., Harlan, S.S., Schulze, B., Finn, C.A., 2007. The floor of Yellowstone Lake is anything but quiet – new discoveries from high-resolution sonar imaging, seismic-reflection profiling, and submersible studies. U.S. Geological Survey Professional Paper 1717, pp. 95–128.

Morgan, L.A., Shanks III, W.C., Pierce, K.L., 2009. Hydrothermal processes above the Yellowstone magma chamber – large hydrothermal systems and large hydrothermal explosions. Geol. Soc. Am. Spec. Pap. 459, 1–95.

Nuti, S., Noto, P., Ferrara, G.C., 1980. The system H_2O-CO_2-CH_4-H_2 at Travale, Italy: Tentative interpretation. Geothermics 9, 287–295.

Panichi, C., Ferrara, G.C., Gonfiantini, R., 1977. Isotope geothermometry in the Larderello geothermal field. Geothermics 5, 81–88.

Peterson, D.A., Boughton, G.K., 1998. Organic compounds and trace elements in fish tissue and bed sediment from streams in the Yellowstone river basin, Montana and Wyoming, 1998. U.S. Geological Survey Water-Resources Investigations Report 00-4190, pp. 1–39.

Podera, R.J., Craig, H., Arnorsson, S., Welhan, J.A., 1992. Helium isotopes in Icelandic geothermal systems: I. ^{3}He, gas chemistry and ^{13}C relations. Geochim. Cosmochim. Acta 56, 4221–4228.

Porter, K., Volman, D.H., 1962. Flame ionization detection of carbon monoxide for gas chromatographic analysis. Anal. Chem. 34, 748–749.

Reysenbach, A.L., Ehringer, M.A., Hershberger, K., 2000. Microbial diversity at 83 °C in Calcite Springs Yellowstone National Park, reveals a novel deeply rooted bacterial lineage and another member of the Korarchaeota. Extremophiles 4, 61–67.

Schoell, M., 1983. Genetic characterization of natural gases. Am. Assoc. Pet. Geol. Bull. 67, 2225–2238.

Schoell, M., 1988. Multiple origins of methane in the Earth. Chem. Geol. 71, 1–10.

Schouten, S., van der Meer, M.T.J., Hopmans, E.C., Rijpstra, W.I.C., Reysenbach, A.-L., Ward, D.M., Sinninghe Damsté, J.S., 2007. Archaeal and bacterial glycerol dialkyl glycerol tetraether lipids in hot springs of Yellowstone National Park. Appl. Environ. Microbiol. 73, 6181–6191.

Seewald, J.S., 2001. Aqueous geochemistry of low molecular weight hydrocarbons at elevated temperatures and pressures: constraints from mineral buffered laboratory experiments. Geochim. Cosmochim. Acta 65, 1641–1664.

Shanks III, W.C., Morgan, L.A., Balistrieri, L., Alt, J.C., 2005. Hydrothermal vent fluids, siliceous hydrothermal deposits, and hydrothermally altered sediments in Yellowstone Lake. In: Inskeep, W.P., McDermott, T.R. (Eds.), Geothermal Biology and Geochemistry in Yellowstone National Park. Thermal Biology Institute, Bozeman, Montana, pp. 53–72.

Shanks III, W.C., Alt, J.C., Morgan, L.A., 2007. Geochemistry of sublacustrine hydrothermal deposits in Yellowstone Lake - Hydrothermal reactions, stable-isotope systematics, sinter deposition, and spire formation. In In the Greater Yellowstone Area - Volcanic, Tectonic, and Hydrothermal Processes in the Yellowstone Geoecosystem. U.S. Geological Survey Professional Paper 1717, pp. 201–234.

Sheppard, D.S., Truesdell, A.H., Janik, C.J., 1992. Geothermal gas compositions in Yellowstone National Park, USA. J. Volcanol. Geoth. Res. 51, 79–93.

Sherwood Lollar, B., Westgate, T.D., Ward, J.A., Slater, G.F., Lacrampe-Couloume, G., 2002. Abiogenic formation of alkanes in the Earth's crust as a minor source for global hydrocarbon reservoirs. Nature 416, 522–524.

Sherwood Lollar, B., Lacrampe-Couloume, G., Slater, G.F., Ward, J., Moser, D.P., Gihring, T.M., Lin, L.-H., Onstott, T.C., 2006. Unravelling abiogenic and biogenic sources of methane in the Earth's deep subsurface. Chem. Geol. 226, 328–339.

Simoneit, B.R.T., 1983. Effects of hydrothermal activity on sedimentary organic matter: Guaymas Basin, Gulf of California - petroleum genesis and proto-kerogen degradation. In: Rona, P.A., Boström, K., Laubier, L., Sith, K.L. (Eds.), Hydrothermal Processes at Seafloor Spreading Centers. Springer, Plenum Press, New York, USA, pp. 451–471.

Simoneit, B.R.T., Lonsdale, P.F., 1982. Hydrothermal petroleum in mineralized mounds at the seabed of Guaymas Basin. Nature 295, 198–202.

Sohn, R.A., Luttrell, K., Shroyer, E., Stranne, C., Harris, R.N., Favorito, J.E., 2019. Observations and modeling of a hydrothermal plume in Yellowstone Lake. Geophys. Res. Lett. 46, 6435–6442.

Tan, C., Cino, C.D., Ding, K., Seyfried Jr., W.E., 2017. High temperature hydrothermal vent fluids in Yellowstone Lake: Observations and insights from in-situ pH and redox measurements. J. Volcanol. Geoth. Res. 314, 263–270.

Tan, C., Fowler, A.P.G., Tudor, A., Seyfried Jr., W.E., 2020. Heat and mass transport in sublacustrine vents in Yellowstone Lake, Wyoming: In-situ chemical and temperature data documenting a dynamic hydrothermal system. J. Volcanol. Geoth. Res. 405, 107043.

Tudor, A., Fowler, A.P.G., Foustoukos, D.I., Moskowitz, B., Wang, L., Tan, C., Seyfried Jr., W.E., 2021. Geochemistry of vapor-dominated hydrothermal vent deposits in Yellowstone Lake, Wyoming. J. Volcanol. Geoth. Res. 414, 107231.

Walker, J.J., Spear, J.R., Pace, N.R., 2005. Geobiology of a microbiol endolithic community in the Yellowstone geothermal environment. Nature 434, 1011–1014.

Wang, D.T., Gruen, D.S., Sherwood Lollar, B., Hinrichs, K.-U., Stewart, L.C., Holden, J.F., Hristov, A.N., Pohlman, J.W., Morrill, P.L., Konneke, M., Delwiche, K.B., Reeves, E. P., Sutcliffe, C.N., Ritter, D.J., Seewald, J.S., McIntosh, J.C., Hemond, H.F., Kubo, M. D., Cardace, D., Hoehler, T.M., Ono, S., 2015. Nonequilibrium clumped isotope signals in microbial methane. Science 348, 428–431.

Wang, D.T., Reeves, E.P., McDermott, J.M., Seewald, J.S., Ono, S., 2018. Clumped isotopologue constraints on the origin of methane at seafloor hot springs. Geochim. Cosmochim. Acta 223, 141–158.

Welhan, J.A., 1988. Origins of methane in hydrothermal systems. Chem. Geol. 71, 183–198.

Werner, C., Brantley, S., 2003. CO_2 emissions from the Yellowstone volcanic system. Geochem. Geophys. Geosyst. 4, 1–27.

White, D.E., Hutchinson, R.A., Keith, T.E.C., 1988. Geology and remarkable thermal activity of Norris Geyser Basin, Yellowstone National Park, Wyoming. U.S. Geological Survey Professional Paper 75, pp. 1–84.

Whiticar, M.J., 1990. A geochemical perspective of natural gas and atmospheric methane. Org Geochem. 16, 531–547.

Yang, T., Lyons, S., Aguilar, C., Cuhel, R., Teske, A., 2011. Microbial communities and chemosynthesis in Yellowstone Lake sublacustrine hydrothermal vent waters. Front. Microbiol. 2, 1–17.